CHAPTER 9

Fs-Laser Scissors for Photobleaching, Ablation in Fixed Samples and Living Cells, and Studies of Cell Mechanics

Alexander Heisterkamp,[⋆] Judith Baumgart,[⋆] Iva Z. Maxwell,[†] Anaclet Ngezahayo,[‡] Eric Mazur,[†] and Holger Lubatschowski[⋆]

[⋆]Laser Zentrum Hannover, Hollerithallee 8, D-30419 Hannover, Germany

[†]Department of Engineering and Applied Science, Harvard University, Cambridge, Massachusetts 02138

[‡]Institute of Biophysics, Leibniz University Hannover, D-30419 Hannover, Germany

The use of ultrashort laser pulses for microscopy has steadily increased over the past years. In this so-called multiphoton microscopy, laser pulses with pulse duration around 100 femtoseconds (fs) are used to excite fluorescence within the samples. Due to the high peak powers of fs lasers, the absorption mechanism of the laser light is based on nonlinear absorption. Therefore, the fluorescence signal is highly localized within the bulk of biological materials, similar to a confocal microscope. However, this nonlinear absorption mechanism can not only be used for imaging but for selective alteration of the material at the laser

METHODS IN CELL BIOLOGY, VOL. 82
Copyright 2007, Elsevier Inc. All rights reserved.

0091-679X/07 $35.00
DOI: 10.1016/S0091-679X(06)82009-1

focus: The absorption can on one hand lead to the excitation of fluorescent molecules of fluorescently tagged cells by the simultaneous absorption of two or three photons or on the other hand, in case of higher order processes, to the creation of free-electron plasmas and, consequently, plasma-mediated ablation. Typical imaging powers are in the range of tens of milliwatts using 100-fs pulses at a repetition rate of 80–90 MHz, while pulse energies needed for ablation powers are as low as a few nanojoules when using high numerical aperture microscope objectives for focusing the laser radiation into the sample.

Since the first demonstration of this technique, numerous applications of fs lasers have emerged within the field of cellular biology and microscopy. As the typical wavelengths of ultrashort laser systems lie in the near infrared between 800 and 1000 nm, high penetration depth can be achieved and can provide the possibility of imaging and manipulating the biological samples with one single laser system.

I. Introduction

Ultrashort laser pulses can lead to very high peak power up to the TW/cm^2, when the laser radiation is focused by high numerical aperture (NA) objectives. These high peak intensities can be used to induce nonlinear absorption effects at the focus region, even in materials that are under one-photon conditions transparent, confining the interaction to very small volumes of only a few femtoliters. As a consequence, two main applications of ultrashort laser pulse have evolved over the past years, imaging, for example multiphoton microscopy, as first realized in living cells by Denk *et al.* (1990), and micromachining within the bulk of different materials by plasma-mediated ablation, as used by Stern *et al.* (1989) and Juhasz *et al.* (1999), to ablate corneal tissue or even bulk materials like fused silica (Chichkov *et al.*, 1996; Schaffer *et al.*, 2001). In multiphoton microscopy, the laser beam is scanned within the biological sample, inducing the excitation of fluorescent molecules by the simultaneous absorption of two or three photons. The image is reconstructed by collecting the induced fluorescence spot by spot, analogue to confocal microscopy.

For these imaging purposes the average laser powers are typically in the range of several milliwatts up to tens of milliwatts, when focusing with objectives of 0.8 or higher NA. When higher laser power is applied, an interplay of multiphoton absorption and cascade ionization, induced by absorption of inverse bremsstrahlung, leads to the creation of high-density plasmas, which results in a very precise and localized plasma-mediated ablation of the material at the laser focus (Vogel and Venugopalan, 2003).

The first group to use short pulses for micro ablation was Michael Berns in the late 1980s or early 1990s (Berns *et al.*, 1981; Tao *et al.*, 1988). In the following years, various applications of laser microbeams in cell biology evolved, as for example the precise dissection of chromosomes (Djabali *et al.*, 1991; Liang *et al.*, 1993; Monajembashi *et al.*, 1986).

Fs lasers have been introduced to cellular dissection by Karsten Koenig by demonstrating as well the dissection of chromosomes in a living cell (Koenig *et al.*, 1999).

While studying the side effects of ultrashort pulse illumination of biological samples, he found that after exceeding a certain threshold, very precise ablation within the bulk of the sample is possible, coining the term nanosurgery. Nowadays, fs lasers are increasingly used to micromanipulate and ablate nanoscale structures in living cells, for example dissection and precise ablation of chromosomes (Koenig, 2000) or ablation of single organelles like mitochondria (Shen *et al.*, 2005; Watanabe *et al.*, 2004). In another application, fs-laser pulses can be used to selectively transfect cells with foreign DNA as shown by Tirlapur and Koenig (2002).

In contrast to UV-laser scissors, the application of fs-laser systems, which can achieve a comparable cutting precision within biological samples (Aist *et al.*, 1993; Stern *et al.*, 1989), offers two main advantages: First, the ablation mechanism is based on nonlinear absorption, allowing the precise ablation of subcellular components deep inside the bulk of tissue or cell cultures. Although ns or ps pulses can be employed for multiphoton absorption as well, the energy delivered to the sample can be minimized by using ultrashort laser pulses (Vogel and Venugopalan, 2003), reducing mechanical and thermal side effects. By fine-tuning of the parameters, ablation dimensions below 100 nm are achievable (Koenig, 2000), leading to the term nanoscissors. As the wavelength of an ultrashort laser is typically in the near infrared, for example centered at 800 nm, high penetration depths of up to several hundreds of micrometers into tissues are possible (So *et al.*, 1998). The amount of laser radiation which is absorbed in regions outside the focus is negligible. Thus, applications even in whole organisms, like *Caenorhabditis elegans* (Chung *et al.*, 2005; Yanik *et al.*, 2004), and drosophila embryos (Supatto *et al.*, 2005), or even working in the brains of living rats (Nishimura *et al.*, 2006) become possible. The second advantage is the possible combination of imaging and ablation, as one fs-laser system can be used simultaneously for both imaging and cutting of cellular samples. Moreover, the nonlinear nature of the optical absorption allows the treatment of any transparent sample, regardless of its linear absorption coefficient as the multiphoton absorption is limited to the focus region. With pulse duration of about 100 fs, only a few nanojoules of energy are necessary to achieve ablation. As possibly harmful effects like cavitation and heat deposition scale with the amount of applied laser energies (Vogel *et al.*, 2005), ultrashort laser applications offer a way to manipulate live cells with very low side effects, the low energy limits collateral damage to the very vicinity of the laser focus and reduces the possibility that the cells will be injured or killed.

II. Methods

A. Optical Setup

Since the laser pulse energies needed to achieve a breakdown are low compared to the typical output powers of standard fs-laser systems, so-called oscillator laser systems with repetition rates of 80–90 MHz and pulse energies of several nanojoules are usually used. Thus, the laser power of such systems is typically several

hundreds of milliwatts. Our laser system (Coherent Chameleon) emits laser pulses of 140-fs pulse duration and allows the tuning of the wavelength of the laser between 715 and 955 nm. The laser radiation is coupled into a microscope objective, for example a Zeiss Achroplan C water immersion objective with an NA of 0.8, focusing the laser beam to a theoretical spot size of roughly 600 nm at a wavelength of 800 nm. As the laser threshold for inducing multiphoton processes is intensity dependent, the pulse duration should be kept as low as possible, leading to a minimum amount of energy delivered to the sample, minimizing the collateral damage to the sample. Moreover, one has to adjust the laser parameters correctly, as laser parameters like repetition rate and pulse energy are very sensitive with respect to the collateral damage within the sample. At high repetition rates, pulse-to-pulse interaction can lead to heat accumulation within the sample, as observed in fused silica (Schaffer *et al.*, 2001). Therefore, the application of MHz pulses for cutting has to be controlled by a fast shutter, preventing the heating of the sample by consecutive pulses, or by an acousto-optic modulator to lower the repetition rates to the kHz regime. Additionally, nonlinear propagation effects inside the objective and the sample can stretch the pulse duration, making pulse width well below 100 fs not well usable. The dispersion of our objective leads to an effective pulse duration inside the sample of roughly 220 fs (Koenig, 2000).

In our setup, the laser radiation is guided over a computer-controlled scanning system (Cambridge Technologies, MA, 6210) for acquiring multiphoton images with the possibility of synchronous ablation by a second laser beam. The setup is shown in Fig. 1. An acousto-optic modulator (by APE, Berlin, Pulse Select) is used to divide the repetition rate in the cutting beam down to kHz, whereas the zero-order diffracted beam is used for multiphoton imaging. This imaging beam is directed over the scanning mirrors to scan the laser beam over the back aperture of the objective. The image acquisition and scanner system is computer controlled by a LabView program described by Tsai *et al.* (2002). The setup for the multi-photon imaging consists of different dichroic mirrors and a photomultiplier tube (Hamamatsu, R6357, Japan) for the detection of the fluorescence and a CCD camera for white light images. Additionally, a UV lamp offers the possibility of acquiring conventional fluorescence images. The second laser beam, the cutting beam, could be whether chosen to be fixed, taking continuously multiphoton images, or it could be guided over the scanning mirrors, allowing more complicated cutting pattern or to target multiple points within the sample. A three-dimensional (3D) computer-controlled positioning of the sample is enabled by a piezo-controlled positioning stage (Thorlabs Inc., NJ, Nanomax 311) with a resolution of 20 nm.

B. Cell Preparation

Bovine capillary endothelial (BCE) cells (passage 10–15) were maintained at 37 °C in 5% CO_2 on tissue culture dishes in a complete medium composed of low-glucose Dulbecco's modified Eagle's medium (DMEM; Gibco-BRL, Grand Island, NY) supplemented with 10% fetal calf serum (FCS) (Hyclone, Logan, Utah),

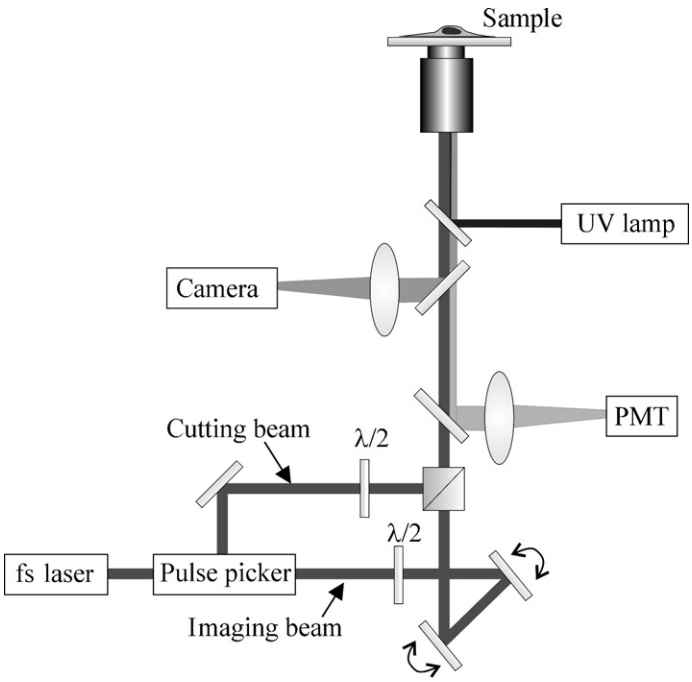

Fig. 1 The laser radiation is guided in two paths toward the objective, an imaging path at 90-MHz repetition rate and at low power, the other path at higher powers and low repetition rates for disruption of organelles. The half wave plates are used in combination with beam splitter cubes to attenuate the laser beams.

10-mM HEPES (JRH-Biosciences, Lenexa, KS), and glutamine (0.292 mg/ml)/penicillin (100 U/ml)/streptomycin (100 g/ml) as previously described by Kumar *et al.* (2006). The granulosa cells were cultivated the same way and were labeled, for the live-cell experiments targeting the mitochondria, with 1-mmol/liter MitoTracker Orange buffered solution (Invitrogen GmbH, Karlsruhe, Germany), compounded with dimethylsulfoxide (DMSO). The dye was added to the nutrient solution at the rate of 1:500 for 45 min. The linear absorption maximum of MitoTracker Orange is at 554 nm and the emission maximum is at 576 nm.

The rat fibroblasts were resistant for 5-bromo-2′-deoxyuridine. The cells were incubated for 10 min with 1.7 μg/ml DAPI (4′,6-diamidino-2-fenipentol) to label the cell nucleus. The linear absorption maximum of DAPI is at 358 nm and the emission maximum is at 461 nm.

For the live-cell experiments targeting the cytoskeleton, cells were transfected for 48 h with an adenoviral vector system encoding enhanced green fluorescent protein (EGFP)-tagged G-tubulin (for microtubules) or with yellow fluorescent protein (YFP)-tagged G-actin (for actin fibers), trypsinized (Trypsin-EDTA, Gibco by Invitrogen GmbH, Karlsruhe, Germany), harvested, and seeded onto glass-bottomed

35-mm dishes (MatTek, Ashland, MA) in complete medium. Prior to imaging, cells were transferred into a nonfluorescent, CO_2-independent medium (pH 7.3) containing (in mM): $CaCl_2$ (1.26), $MgSO_4$ (0.81), KCl (5.36), KH_2PO_4 (0.44), NaCl (137), Na_2HPO_4 (0.34), D-glucose (5.55), L-glutamine (2.0), sodium pyruvate (1.0), HEPES (20.0), 1% bovine serum albumin, 10% calf serum, and MEM essential and nonessential amino acids (Sigma, St. Louis, MO).

For the transmission electron microscopy (TEM) experiments with fixed cells, the cells were then trypsinized (Trypsin–EDTA, Gibco), harvested, and seeded onto -carbon-coated formvar on Embra TEM finder grids (Electron Microscope Sciences, PA) in complete medium. After allowing the cells to attach and spread for 12–24 h, the cells were fixed in 4% formaldehyde (electron microscopy grade) in phosphate buffered saline (PBS) for 40 min, permeabilized in 0.1% Triton X-100 in PBS for 5 min, blocked in 1% bovine serum albumin in PBS for 1 h, and stained for either actin (Alexa Fluor488 phalloidin, Molecular Probes, Eugene, OR) or nuclear DNA (Hoechst 33348, Molecular Probes), all at room temperature. Afterward the cells were stored and treated in an aqueous solution (PBS). Following laser treatment, cells were fixed in 2.5% glutaraldehyde in 0.1-M cacodylate buffer, pH 7.4, at 4°C for 1 h and then washed and stored in this buffer at 4°C until processing. Prior to TEM imaging with a Philips CM-10 microscope, cells were fixed in 1% osmium tetroxide in 0.1-M cacodylate buffer, pH 7.4, at 4°C for 30 min, washed in the same buffer, dehydrated in graded ethanol solutions, critical point dried, and carbon coated.

III. Ablation and Photobleaching in Fixed Samples

As cells and cell organelles are typically visualized by fluorescent tagging of the areas of interest, it is important to prove that the laser energy applied to the cellular sample actually cuts or ablates the targeted structure and not only photobleaches the fluorescent dye. Therefore, we performed studies on fixed bovine endothelial cells and rat1 fibroblasts, by cutting within the cytoskeleton stained by actin (endothelial cells) or by ablating within the nucleus of the cell, stained by Hoechst 33348 (endothelial cells) or by DAPI (rat1 fibroblasts).

Figure 2 shows the fluorescence from the actin network within an endothelial cell after it has been irradiated along five parallel lines with various pulse energies (Heisterkamp *et al.*, 2005). The sample was translated at a speed of ~0.7 μm/s corresponding to roughly 15,000 pulses per line. The image shows that the fluorescence intensity following irradiation depends strongly on pulse energy. At 1.8 nJ, the effect of irradiation is barely visible in the fluorescence image, see fluorescence intensity plot in small inset of Fig. 2. Increasing the pulse energy to 2.2 nJ produces a clear decrease in fluorescence with a width of 240 nm. At higher energy, the width of this decrease in fluorescence scales with pulse energy from 360 nm at 2.8 nJ to 500 nm at 3.5 nJ and 600 nm at 4.4 nJ.

Similar results and thresholds for laser ablation are found in rat1 fibroblast, when targeting the cells' nucleus. Figure 3A shows the nucleus of a fixed

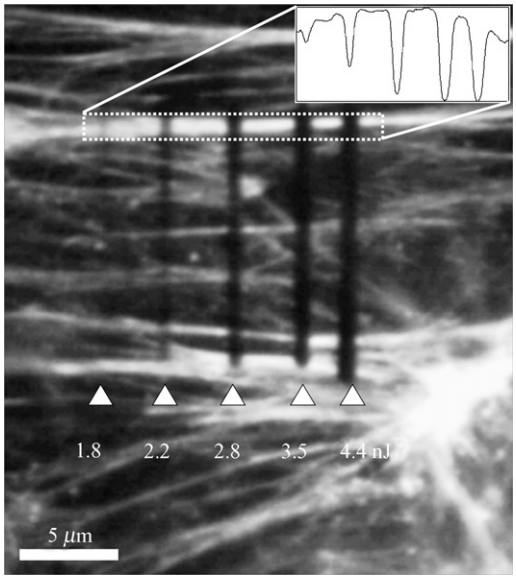

Fig. 2 Fluorescence microscope image of laser cuts through YFP-labeled actin fibers in a fixed endothelial cell obtained by irradiation (Heisterkamp *et al.*, 2005).

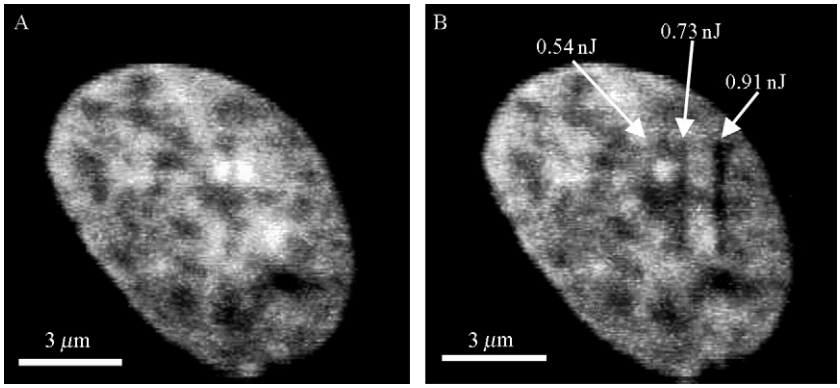

Fig. 3 Fixed rat1 fibroblast, the nucleus is DAPI labeled. (A) The nucleus before manipulation and (B) the same nucleus after manipulation by different pulse energies: 0.54, 0.73, and 0.91 nJ. The images were taken by two-photon microscopy.

fibroblast, stained by DAPI for nuclear DNA. After applying the laser pulses at three different energies of 0.54, 0.73, and 0.91 nJ, ablated channels within the nucleus can be seen, Fig. 3B, showing a clear line at 0.91 nJ, a faint cut at 0.73 nJ, and no change in fluorescence at 0.54 nJ.

To determine the onset of plasma-mediated ablation from the threshold for laser-induced bleaching of the dyes, we compared fluorescent micrographs of laser-irradiated cells with images taken by TEM. Figure 4A shows the fluorescence image of the nucleus of an endothelial cell, stained by Hoechst 33348, with laser cuts at 1.45, 1.8, and 2.3 nJ. Again, the thickness and visibility of the cut scales with laser intensity. In Fig. 4B, the same nucleus is shown in TEM. Apparently, the faint cut at 1.45 nJ is not visible in the TEM, thus, the observed line in Fig. 4A must be due to photobleaching.

At higher energies, clear cuts can be seen in both images, see cuts at 1.8 and 2.3 nJ. The data allow us to define three regimes of irradiation: no interaction (no damage visible in either image), photobleaching without material loss (only the fluorescence image shows a change), and ablation of material (both images show cuts). For pulse energies above 10–15 nJ, a much larger part of the cell is ablated (not shown) most likely due to cavitation. Part of the energy delivered to the sample cannot be dissipated through thermal diffusion, producing rapid, local increase in material temperature, leading to an explosive expansion of the material and, thus, damage far from the laser focus (Vogel *et al.*, 2005).

Although the thresholds vary from sample to sample and especially from dye to dye, see for comparison thresholds in Figs. 2 and 3, we found the energy threshold of ablation to be at most 20% higher than the photobleaching threshold. In other words, if energies exceed 1.2 times the threshold at which fluorescence disappears, one can be assured of ablation. The TEM and fluorescence microscopy measurements reveal that the ablation width depends strongly on pulse energy, with pulse energies between 1.2 and 1.7 nJ producing material loss as small as 200 nm. Above

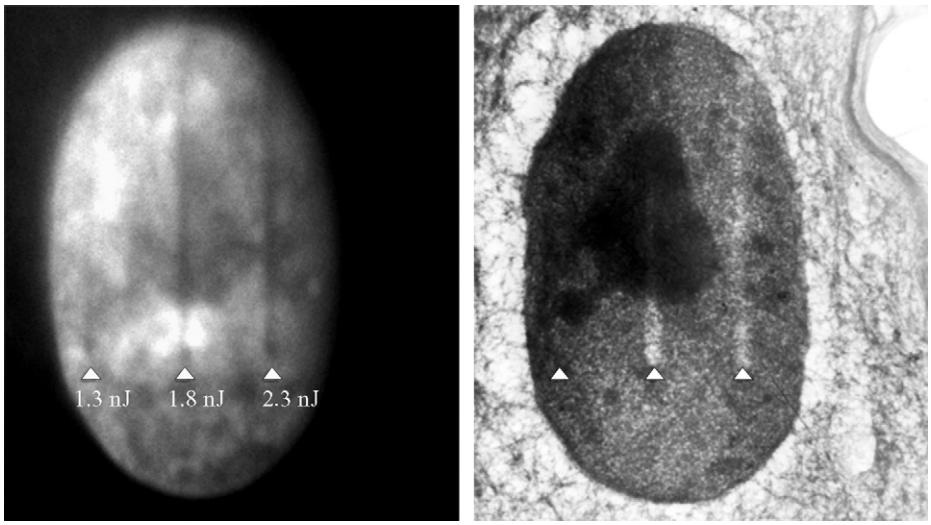

Fig. 4 Fluorescent (A) and transmission electron microscopy (B) images of the same nucleus of a bovine endothelial cell, processed by fs laser (Heisterkamp *et al.*, 2005).

1.7 nJ, the ablation width increases with energy; around 3 nJ the ablation width is ~1 mm. If such energies are applied to live cells, micromanipulation at resolution below a micrometer within the cells is possible.

IV. Applications in Living Cells

A. Cell Organelle Ablation

Once the thresholds for ablation in fixed cells are established, one can move to living cells and target submicron regions inside a single cell. In a first set of experiments, we targeted mitochondria in endothelial cells and granulosa cells stained by MitoTracker Orange to study the induction of cell death, so-called apoptosis. Imaging the cell's reaction to the disruption by multiphoton microscopy imparts information about the sequences of intracellular processes. In order to observe the viability of the cell in dependence to mitochondria disruption, the cell had to be observed over a longer period up to 1 h with both fluorescence imaging and bright field microscopy imaging. The mitochondria disruption was realized at pulse energies between 0.7 and 1.0 nJ and with a speed of ~14 μm/s at a repetition rate of the cutting beam of 90 MHz. The reaction of the cell was observed by comparing the images before and after manipulation.

Typically, a cell changes its volume when it initiates apoptosis and forms vesicles within its volume, which can be seen in the bright field microscopy image and in the fluorescence image by an important change of the mitochondria arrangement. Figure 5A shows living endothelia cells whose mitochondria are MitoTracker

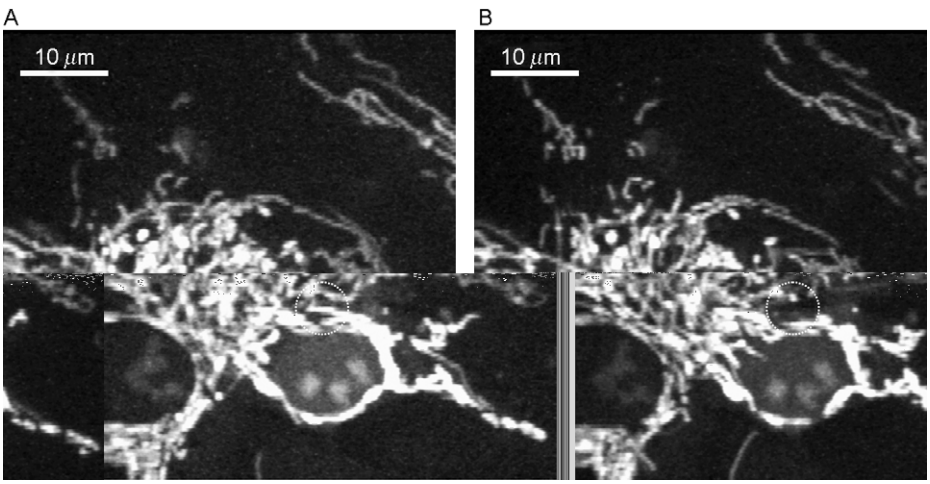

Fig. 5 MitoTracker Orange labeled endothelia cells before (A) and after (B) manipulation. The mitochondrion pointed highlighted by the circle was disrupted at a pulse energy of 1 nJ. Images were taken by two-photon microscopy, in parallel to the laser cutting.

Orange labeled. In Fig. 5B, the ablation of a single mitochondrion (see circle) was realized at pulse energies of 1 nJ.

In none of our studies, the ablation of a single mitochondrion led to the induction of cell death. Apparently, to induce cell death, one has to severe multiple mitochondria. Thus, we targeted several mitochondria within different granulosa cells, as displayed in Fig. 6, showing two cells before ablation (A), the targeted mitochondria (B) within the cells and after ablation (C). Figure 6D provides a white light image of the two cells. The difference in the fluorescence image between Fig. 6A and C is shown in Fig. 6E by digital subtraction of the images. Clearly, the areas of targeted ablation coincide with the areas of change in fluorescence, although some changes outside the laser manipulation are visible, likely due to movement of the cell and reorganization of the mitochondria network. To further investigate the process of apoptosis, a LabView program to target the mitochondria in the whole cell in 3D is currently developed and further studies comparing cancerous with healthy cells are underway.

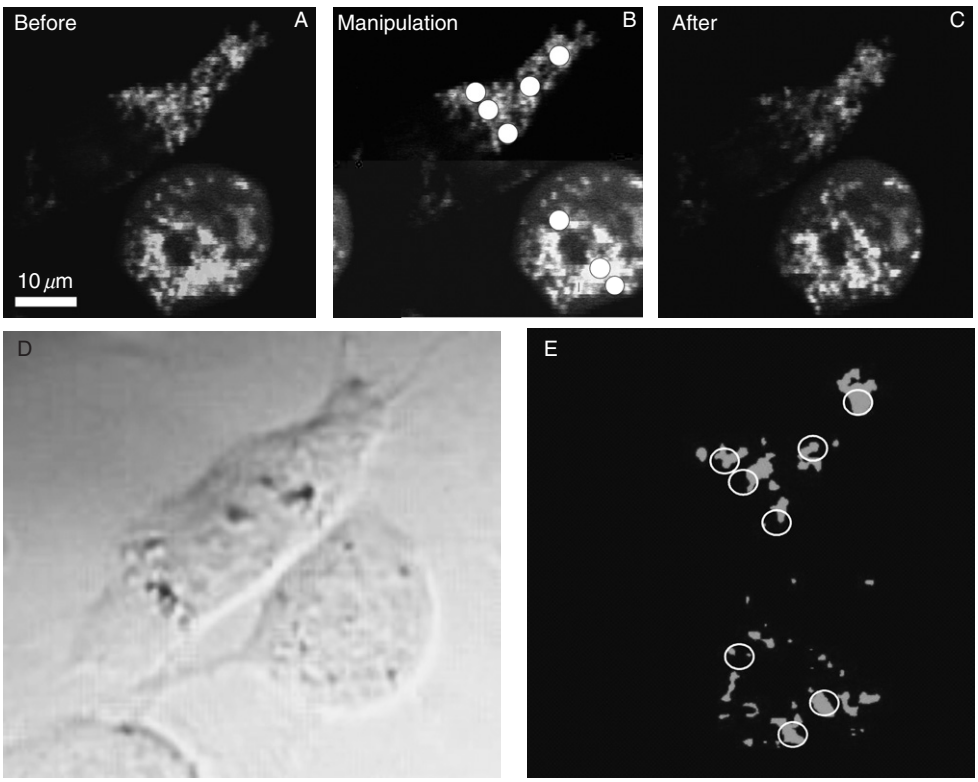

Fig. 6 Multiphoton microscope images of two granulosa cells by MitoTracker Orange. (A) Before laser irradiation, (B) laser-targeted mitochondria, (C) after laser irradiation. (D) White light image of the cells, (E) digital subtraction of (A) and (C).

B. Cell Mechanics

Another application of fs-laser scissors in cell biology is cell mechanics, meaning the manipulation at parts of the cytoskeleton of a cell in order to gather more information about the structural integrity and mechanical stress and tension within a cell. Thus, we tried to cut single microtubules in a live bovine endothelial cell. Microtubules consist of protein subunits of tubulin, which form a stiff hollow tube with typical diameters of about 25–30 nm and length of up to several 10 μm and are part of the cytoskeleton. If such a structure is cut by a laser, it depolymerizes rapidly due to its dynamic instability. This can be seen by the fluorescence microscopy images in Fig. 7 (Heisterkamp *et al.*, 2005). The laser was aimed at a curved

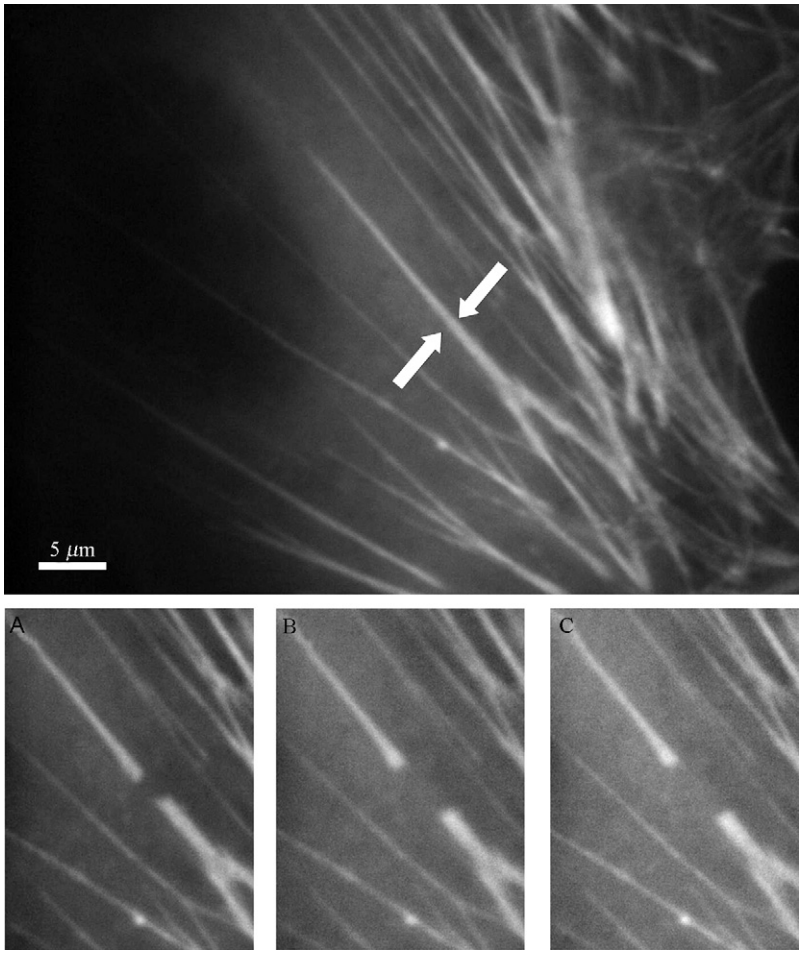

Fig. 7 Cuts in the cytoskeleton of a live endothelial cell stained by YFP for actin taken fluorescent microscopy. Cell before and after laser cutting (A) = 0.5 s, (B) = 5 s, and (C) = 7.5 s, showing the retraction of the fiber ends.

microtubule in the middle of the image (see arrow), lying above the cells' nucleus (dark area in the image). After cutting, both ends of the microtubule snapped back and started to depolymerize, as shown in the right of Fig. 7, taken ~16 s after the laser cut. Both ends of the microtubule are already several micrometers apart, proving that the microtubule is clearly cut. Nevertheless, other microtubules close to the ablation site stay intact, showing the very low side effects of fs-laser ablation.

In a different set of experiments, we tried to target the actin fiber network of the BCE cells, which form another part of the cytoskeleton and are assumed to bear tension. Many measurements of the mechanical properties of these stress fibers have already been done *in vitro*; however, there has been no tool to probe the physical properties of actin fibers in their natural environment. We aimed the fs laser at a single fiber and measured its retraction after cutting. Figure 8 displays a time lapse of the stress fiber before and at 0.5 s (A), 5 s (B), and 7.5 s (C) after laser application. After the dissection of the fiber, both ends snap back in a rapid movement due to the tension resting on the fiber and slowing down until reaching their end position several micrometers apart from the half-micrometer-wide laser spot. By fitting mechanical models to the amount of retraction and imaging the change in shape of the whole cell, information about the tension within a single actin fiber and within the actin network of a cell can be gathered (Kumar *et al.*, 2006).

V. Summary

In this chapter, we have summarized several applications of fs-laser nanoscissors in the field of biology. Comparing fluorescent images with TEM images, it is important to note that the threshold for ablation is roughly 20% higher than the threshold for photobleaching. Thus, laser energies clearly above the notice of a visible effect in fluorescent microscopy should be chosen to ablate structures within living cells. However, the side effects and cutting dimensions scale with the amount of laser energy applied to the target, providing highest precision close to the ablation threshold. The achievable cutting precision is in the range of 200 nm at pulse energy of ~1 nJ. One major advantage of fs-laser systems is their possible combination or integration into multiphoton imaging system, allowing the simultaneous manipulation and imaging by a single laser. However, as a disadvantage, the current cost of an fs-laser system remains quite high when compared to ns- or ps-laser systems. Thus, the use of fs-laser systems is often limited to groups, which are already equipped with a multiphoton microscope and which are using the fs-laser cell surgery as an additional feature of their microscope. Moreover, the minimized side effects of fs-laser systems are not necessary in various applications of cell biology and lower survival rates are quite acceptable, as for example shown by Paterson *et al.* (2006), by successfully transfecting Chinese hamster ovarian cells using a simple violet diode laser. Nevertheless, the application of multiphoton microscope systems is rapidly growing and the development of low-cost fs-laser systems remains an ongoing process, which is why the use of fs-laser systems in cell biology will probably steadily increase in the near future.

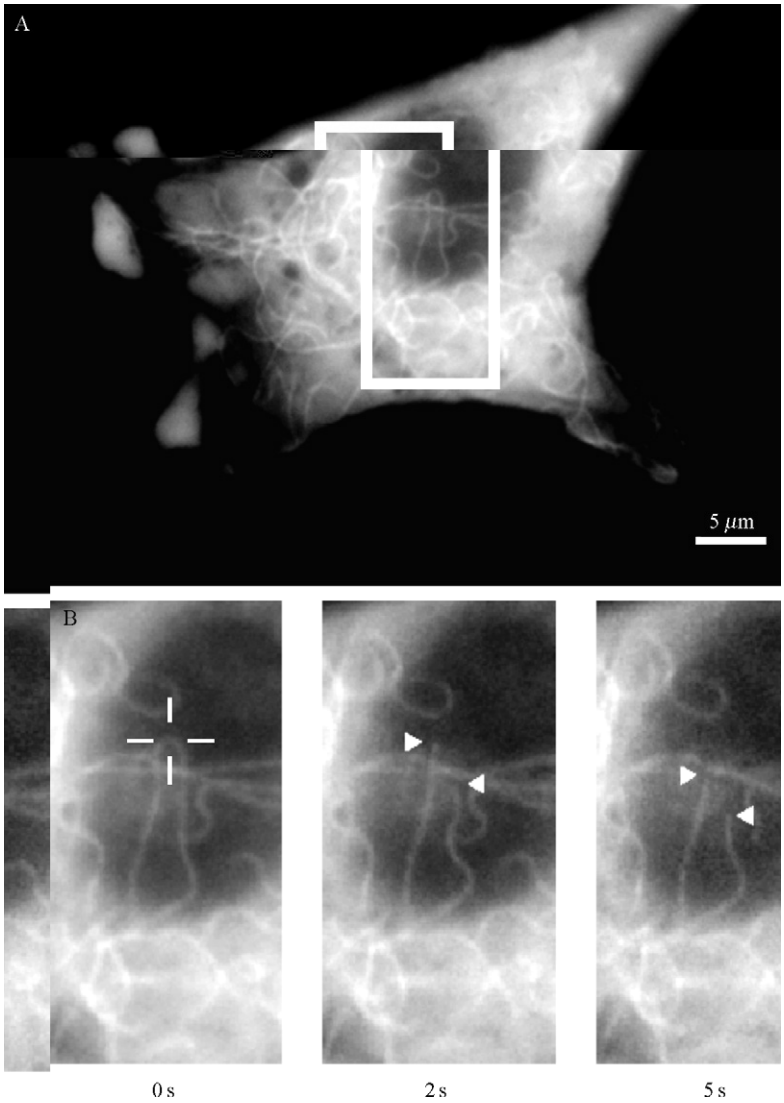

Fig. 8 (A) Fluorescence microscope image of GFP-labeled microtubule network in an endothelial cell. (B) Time-lapse sequence showing rapid retraction of microtubule due to depolymerization. The cross hair shows the position targeted by the laser; the triangles show the retracting ends of the microtubule.

However, open question remains, concerning the optimum repetition rate of such fs-laser scissors, as the basic mechanism of plasma-mediated ablation and possible pulse-to-pulse interaction are topic of actual discussions.

Acknowledgments

The author would like to thank the editors of this book for the helpful comments on the manuscript. Parts of this work were funded by the Deutsche Forschungsgemeinschaft (DFG). The author has no financial or proprietary interest in any of the procedures or devices used in this chapter.

References

Aist, J. R., Liang, H., and Berns, M. W. (1993). Astral and spindle forces in PTK2 cells during anaphase B: A laser microbeam study. *J. Cell Sci.* **104,** 1207–1216.

Berns, M. W., Aist, J., Edwards, J., Strahs, K., Girton, J., McNeil, P., Rattner, J. B., Kitzes, M., Hammerwilson, M., Liaw, L. H., Slemens, A., Koonce, M., *et al.* (1981). Laser microsurgery in cell and developmental biology. *Science* **213,** 505–513.

Chung, S. H., Clark, D. A., Gabel, C. V., Mazur, E., and Samuel, A. (2005). The role of the AFD neuron in *C. elegans* thermotaxis analyzed using femtosecond laser ablation. *BMC Neurosci.* **7,** 30.

Chichkov, B., Momma, C., Nolte, S., von Alvensleben, F., and Tuennermann, A. (1996). Femtosecond, picosecond and nanosecond laser ablation. *Appl. Phys. A* **63,** 109–115.

Denk, W., Strickler, J. H., and Webb, W. W. (1990). Two-photon laser scanning fluorescence microscopy. *Science* **248,** 73–76.

Djabali, M., Nguyen, C., Biunno, I., Oostra, B. A., Mattei, M. G., Ikeda, J. E., and Jordan, B. (1991). Laser microdissection of the fragile X region: Identification of cosmid X clones and of conserved sequences in this region. *Genomics* **10,** 1053–1060.

Heisterkamp, A., Maxwell, I. Z., Mazur, E., Underwood, J. M., Nickerson, J. A., Kumar, S., and Ingber, D. E. (2005). Pulse energy dependence of subcellular dissection by femtosecond laser pulses. *Opt. Express* **13,** 3690–3696.

Juhasz, T., Loesel, F. H., Kurtz, R. M., Horvath, C., Bille, J. F., and Mourou, G. (1999). Corneal refractive surgery with femtosecond lasers. *IEEE J. Sel. Top. Quantum Electron.* **5**(4), 902–910.

Koenig, K. (2000). Multiphoton microscopy in life sciences. *J. Microsc.* **200,** 83–104.

Koenig, K., Riemann, I., Fischer, P., and Halbhuber, K. (1999). Intracellular nanosurgery with near infrared femtosecond laser pulses. *Cell. Mol. Biol.* **45,** 192–201.

Kumar, S., Maxwell, I. Z., Heisterkamp, A., Polte, T. R., Lele, T. P., Salanga, M., Mazur, E., and Ingber, D. E. (2006). Viscoelastic retraction of single living stress fibers and its impact on cell shape, cytoskeletal organization, and extracellular matrix mechanics. *Biophys. J.* **90,** 3762–3773.

Liang, H., Wright, W. H., Cheng, S., He, W., and Berns, M. W. (1993). Micromanipulation of chromosomes in PTK2 cells using laser microsurgery (optical scalpel) in combination with laser induced optical force (optical tweezers). *Exp. Cell Res.* **204,** 110–120.

Monajembashi, S., Cremer, S., Cremer, T., Wolfrum, J., and Greulich, K. O. (1986). Microdissection of human chromosomes by a laser microbeam. *Exp. Cell. Res.* **167**(1), 262–265.

Nishimura, N., Schaffer, C. B., Friedman, B., Tsai, P. S., Lyden, P. D., and Kleinfeld, D. (2006). Targeted insult to subsurface cortical blood vessels using ultrashort laser pulses: Three models of stroke. *Nat. Meth.* **3,** 99–108.

Paterson, L., Agate, B., Comrie, M., Ferguson, R., Lake, T. K., Morris, J. E., Carruthers, A. E., Brown, C. T. A., Sibbett, W., Bryant, P. E., Gunn-Moore Riches, F. C., and Dholakia, K. (2006). Photoporation and cell transfection using a violet diode laser. *Opt. Express* **13**(2), 595–600.

Schaffer, C. B., Brodeur, A., Garcia, J. F., and Mazur, E. (2001). Micromachining bulk glass by use of femtosecond laser pulses with nanojoule energy. *Opt. Lett.* **26,** 93–95.

Shen, N., Datta, D., Schaffer, C. B., Le Duc, P., Ingber, D. E., and Mazur, E. (2005). Ablation of cytoskeletal filaments and mitochondria in live cells using a femtosecond laser microscissors. *Mech. Chem. Biosyst.* **2,** 17–26.

So, P. T. C., Kim, H., and Kochevar, I. E. (1998). Two-photon deep tissue *ex vivo* imaging of mouse dermal and subcutaneous structures. *Opt. Express* **3**(9), 339–350.

Stern, D., Schoenlein, R., Puliafito, C., Dobi, E., Birngruber, R., and Fujimoto, J. (1989). Corneal ablation by nanosecond, picosecond, and femtosecond lasers at 532 nm and 625 nm. *Arch Ophthalmol.* **107**(4), 587–592.

Supatto, W., Debarre, D., Moulia, B., Brouzes, E., Martin, J., Farge, E., and Beaurepaire, E. (2005). *In vivo* modulation of morphogenetic movements in *Drosophila* embryos with femtosecond laser pulses. *Proc. Natl. Acad. Sci. USA* **102,** 1047–1052.

Tao, W., Walter, R. J., and Berns, M. W. (1988). Laser-transected microtubules exhibit individuality of regrowth, however most free new ends of the microtubules are stable. *J. Cell Biol.* **107**(3), 1025–1035.

Tirlapur, U. K., and Koenig, K. (2002). Targeted transfection by femtosecond laser. *Nature* **448,** 290–291.

Tsai, P. S., Nishimura, N., Yoder, E. J., White, A., Dolnick, E., and Kleinfeld, D. (2002). Principles, design and construction of a two photon scanning microscope for *in vitro* and *in vivo* studies. *In* "Methods for *In Vivo* Optical Imaging" (R. Frostig, ed.), pp. 113–171. CRC Press, Boca Raton, Florida.

Vogel, A., and Venugopalan, V. (2003). Mechanisms of pulsed laser ablation of biological tissues. *Chem. Rev.* **103,** 577–644.

Vogel, A., Noack, J., Huettmann, G., and Paltauf, G. (2005). Mechanisms of femtosecond laser nanosurgery of cells and tissues. *Appl. Phys. B* **81**(8), 1015–1047.

Watanabe, W., Arakawa, N., Matsunaga, S., Higashi, T., Fukui, K., Isobe, K., and Itoh, K. (2004). Femtosecond laser disruption of subcellular organelles in a living cell. *Opt. Express* **12,** 4203–4213.

Yanik, M. F., Cinar, H., Cinar, H. N., Chisholm, A. D., Jin, Y., and Ben-Yakar, A. (2004). Neurosurgery: Functional regeneration after laser axotomy. *Nature* **432,** 822.